



OPEN ACCESS

EDITED BY

Yafei Duan,
South China Sea Fisheries Research
Institute, China

REVIEWED BY

Haihui Ye,
Jimei University, China
Xugan Wu,
Shanghai Ocean University, China

*CORRESPONDENCE

Zhaoxia Cui,
cuizhaoxia@nbu.edu.cn

SPECIALTY SECTION

This article was submitted to Aquatic
Physiology,
a section of the journal
Frontiers in Physiology

RECEIVED 27 September 2022

ACCEPTED 17 October 2022

PUBLISHED 31 October 2022

CITATION

Zhu D, Feng T, Mo N, Han R, Lu W,
Shao S and Cui Z (2022), New insights
for the regulatory feedback loop
between type 1 crustacean female sex
hormone (CFSH-1) and insulin-like
androgenic gland hormone (IAG) in the
Chinese mitten crab (*Eriocheir sinensis*).
Front. Physiol. 13:1054773.
doi: 10.3389/fphys.2022.1054773

COPYRIGHT

© 2022 Zhu, Feng, Mo, Han, Lu, Shao
and Cui. This is an open-access article
distributed under the terms of the
[Creative Commons Attribution License
\(CC BY\)](https://creativecommons.org/licenses/by/4.0/). The use, distribution or
reproduction in other forums is
permitted, provided the original
author(s) and the copyright owner(s) are
credited and that the original
publication in this journal is cited, in
accordance with accepted academic
practice. No use, distribution or
reproduction is permitted which does
not comply with these terms.

New insights for the regulatory feedback loop between type 1 crustacean female sex hormone (CFSH-1) and insulin-like androgenic gland hormone (IAG) in the Chinese mitten crab (*Eriocheir sinensis*)

Dandan Zhu¹, Tianyi Feng¹, Nan Mo¹, Rui Han¹, Wentao Lu¹,
Shucheng Shao¹ and Zhaoxia Cui^{1,2*}

¹School of Marine Sciences, Ningbo University, Ningbo, China, ²Laboratory for Marine Biology and Biotechnology, Qingdao National Laboratory for Marine Science and Technology, Qingdao, China

To clarify the hormone control on sex determination and differentiation, we studied the Chinese mitten crab, *Eriocheir sinensis* (Henri Milne Edwards, 1854), a species with importantly economic and ecological significance. The crustacean female sex hormone (CFSH) and the insulin-like androgenic gland hormone (IAG) have been found to be related to the sex determination and/or differentiation. *CFSH-1* of *E. sinensis* (*EsCFSH-1*) encoded a 227 amino-acid protein including a signal peptide, a CFSH-precursor-related peptide, and a mature CFSH peptide. Normally, *EsCFSH-1* was highly expressed in the eyestalk ganglion of adult female crabs, while the expression was declined in the intersex crabs (genetic females). The intersex crabs had the androgenic glands, and the expression level of *EsIAG* was close to that of male crabs. During the embryogenesis and larval development, the changes of *EsCFSH-1* and *EsIAG* genes expression in male and female individuals were shown after the zoea IV stage. Next, we confirmed the existence of the regulatory feedback loop between *EsCFSH-1* and *EsIAG* by RNA interference experiment. The feminization function of *EsCFSH-1* was further verified by examining the morphological change of external reproductive organs after *EsCFSH-1* knockdown. The findings of this study reveal that the regulatory interplay between CFSH and IAG might play a pivotal role in the process of sex determination and/or differentiation in decapod crustaceans.

KEYWORDS

crustacean female sex hormone, insulin-like androgenic gland hormone, intersex crab, early embryogenesis, secondary sexual characteristic, sexual sex differentiation

1 Introduction

The crustacean female sex hormone (CFSH), initially identified in the blue crab, *Callinectes sapidus*, was a neuropeptide hormone synthesized in the X-organ and secreted by the sinus gland in the eyestalk (Zmora and Chung, 2014). Self-explained by its name, the function of CFSH was found to be related to the female sexual sex differentiation of crustaceans, especially the development of the female reproductive anatomies such as gonopores and ovigerous setae (Adkins-Regan, 2014) and possibly the ovarian maturation (Liu et al., 2018; Tsutsui et al., 2018). To date, CFSH has been identified in several crustaceans such as *Carcinus maenas*, *Sagmariasus verreauxi*, *Cherax quadricarinatus*, *Procambarus clarkii*, *Chorismus antarcticus*, *Penaeus japonicus*, *Penaeus monodon*, *Scylla paramamosain*, *Macrobrachium rosenbergii*, and *Lysmata vittata* (Farhadi et al., 2021; Toyota et al., 2021). Nonetheless, the relevant information was lacking in *Eriocheir sinensis*, an economically and ecologically important crustacean.

Discovered in 2007, the insulin-like androgenic gland hormone (IAG) secreted from the androgenic gland (AG) has been proven as a critical peptide hormone regulating male differentiation in decapod species. The masculinizing function of IAG was described as an “IAG-switch” in the endocrine regulatory axis of X-organ-sinus-gland (XO-SG)-androgenic gland (AG)-testis (Levy et al., 2020; Levy and Sagi, 2020). Studies have found that repressing IAG expression at early developmental stages could induce the degeneration of primary and secondary sex characteristics of male, which could eventually lead to feminization (Ventura et al., 2012; Levy et al., 2017; Priyadarshi et al., 2017). To date, IAG orthologs have been identified in several crustacean species, including *Eriocheir sinensis* (Song et al., 2018; Fu et al., 2020; Cui et al., 2021).

CFSH has been regarded as an upstream regulator of IAG, while the recent evidence supported the possible existence of a negative regulatory loop between CFSH and IAG. Previous studies found that CFSH of *Scylla paramamosain* could inhibit the expression of IAG *in vitro* (Liu et al., 2018) and the inhibitory mechanism was later detailed explained (Jiang et al., 2020a; Jiang et al., 2020c), while IAG1 and CFSH of *Lysmata vittata* was able to inhibit the expression of each other reciprocally (Liu et al., 2021b; Liu et al., 2021c). However, the research of the hormone control on sex determination and differentiation has been limited for lacking of sex identification during the embryogenesis and larval development.

In this study, based on the genomic and transcriptomic information, the basic gene feature of CFSH-1 was analyzed in *E. sinensis*. Furthermore, we examined the possibility of existing crosstalk between CFSH-1 and IAG by comparing their expression level at various developmental stages including

distinguished sex embryos and larvae, normal and intersex crabs. At last, we confirmed the regulatory feedback loop by observing the change of gene expression after knocking down its potential inhibitor. The new insights based on the results from embryogenesis and larval individuals and intersex crabs in our study will hopefully contribute to a better understanding of the process of sex determination and differentiation in the Chinese mitten crab and other crustaceans alike.

2 Methods and materials

2.1 Animals and samples

The adults, intersex crabs, larvae and embryos of *E. sinensis* were collected from the local crab farms and hatcheries around Xinghua, Jiangsu province of China. The developmental stages of embryos and larvae were classified according to the previous descriptions (Liang et al., 1974; Montú et al., 1996) under an Olympus BX53F2 stereo microscope (Olympus, Tokyo, Japan). The biological samples were separated in tubes, and rapidly frozen in liquid nitrogen until further usage.

Animal handling and experimental procedures were performed according to the guidelines of the Guide for the Use of Experimental Animals of Ningbo University.

2.2 Total RNA extraction and cDNA synthesis for tissue samples

Total RNA was extracted from tissues including eyestalk ganglion (EG), ovary (O), testis (T), androgenic gland (AG) using

TABLE 1 The summary of primers used in this study.

Primer	Sequence (5'–3')	Application
EsCFSH-1-F	CCTTCTCTTGGGATGTTTCG	Gene cloning
EsCFSH-1-R	ATCTTCACGGCTTGGGTTTC	
EsCFSH-1-qF	ATACGTTGAGCGCCAGATCC	qRT-PCR
EsCFSH-1-qR	CAGAGCCACACATACGGAGC	
EsIAG-qF	GTCCTACAAGCAGCACCC	
EsIAG-qR	AGGGTCTTCCAGATGGATCG	
Es-β-actin-qF	GCATCCACGAGACCACTTACA	
Es-β-actin-qR	CTCCTGCTTGCTGATCCACATC	
EsCFSH-1-dsF	AACCACCATTTGCCATCCCTC	Synthesis of dsRNA
EsCFSH-1-dsR	TTCAGAGCCACACATACGGAG	
EsIAG-dsF	CACCTCATGCAACGTGCAGTT	
EsIAG-dsR	TTCTGCACGTTGCATGAGGTG	
EGFP-dsF	CACAAGTTCAGCGTGTCCG	
EGFP-dsR	AACCACTACCTGAGCACCCA	
Primer-T7	TAATACGACTCACTATAGGG	
Primer-SP6	ATTTAGGTGACACTATAG	

TABLE 2 The source of CFSHs for the multiple sequence alignment and phylogenetic analysis.

Gene name	Species	Genebank accession number or gene ID
<i>SpCFSH-1</i>	<i>Scylla paramamosain</i>	ASU91622.1
<i>SpCFSH-2</i>		ASU91623.1
<i>EsCFSH-1</i>	<i>Eriocheir sinensis</i>	New023086.1
<i>EsCFSH-2a</i>		New 075712.1
<i>EsCFSH-2b</i>		CCG012020.1
<i>CmCFSH-1</i>	<i>Carcinus maenas</i>	AEI72264.0
<i>CmCFSH-2a</i>		GBXE01009034.1
<i>CmCFSH-2b</i>		GBXE01009035.1
<i>PjCFSH-ov</i>	<i>Penaeus japonicus</i>	BBC20727.1
<i>PjCFSH</i>		BBA53799.1
<i>MrCFSH-1a</i>	<i>Macrobrachium rosenbergii</i>	Unigene35740
<i>MrCFSH-1b</i>		Unigene35739
<i>MrCFSH-2a</i>		Unigene35630
<i>MrCFSH-2b</i>		Unigene35631
<i>LyvCFSH-1</i>	<i>Lysmata vittata</i>	QOD42430.1
<i>LyvCFSH-2</i>		QOD42431.1
<i>CsCFSH</i>	<i>Callinectes sapidus</i>	ADO00266.1
<i>PmCFSH</i>	<i>Penaeus monodon</i>	QYK79693.1
<i>PcCFSH-1</i>	<i>Procambarus clarkii</i>	GBEV01018430.1
<i>PcCFSH-2a</i>		GBEV01038769.1
<i>PcCFSH-2b</i>		GBEV01021357.1
<i>LivCFSH-1a</i>	<i>Litopenaeus vannamei</i>	JP398644.1
<i>LivCFSH-1b</i>		JP398645.1
<i>LivCFSH-1c</i>		JP398646.1

the TRIZOL[®] reagent (Invitrogen, California, United States) according to the manufacturer's instructions. The concentration and quality of total RNA were assessed using a NanoDrop One spectrophotometer (Thermo Fisher Scientific, Massachusetts, United States). 1 µg of total RNA was converted to cDNA using the PrimeScript[™] RT reagent Kit with gDNA Eraser (TaKaRa, Tokyo, Japan) following the manufacturer's instructions.

2.3 DNA/RNA co-extraction for embryos and larvae

The DNA/RNA co-extraction was applied for the single embryo at the stages of fertilized egg (Fe), two-cell (2C), and blastula (Bs) and the single larva at the stage of zoea III (Z3), zoea IV (Z4), and zoea V (Z5). Total DNA and RNA of each embryo and larva were extracted simultaneously using a Tiangen DP423 DNA/RNA/Protein Isolation Kit (Tiangen, Beijing, China). Firstly, a specimen was fully homogenized in

the lysis buffer by a Servicebio KZ-III-F low-temperature tissue grinder (Servicebio Technology, Wuhan, China). After leaving on ice for 15 min, the total DNA was separated by centrifuging the lysate through a HiBind[®] DNA mini-column at 13,000 × g for 1 min at room temperature using a Sorvall[™] Legend[™] Micro 17R microcentrifuge (Thermo Fisher Scientific, Waltham, US). After mixing with absolute ethanol and later DNA digestion by DNase I for 15 min, the total RNA in the flow-through lysate was collected by centrifugation through a HiBind[®] RNA mini-column at 13,000 × g for 1 min. Subsequently, the total DNA and RNA were eluted into separated tubes by centrifuging the wash buffer through the columns twice (13,000 × g, 1 min). Finally, the purified nucleic acids were dissolved in 100 µL DEPC-treated water. The concentration and quality of the DNA and total RNA were assessed using a NanoDrop 2000 spectrophotometer (Thermo Fisher Scientific, Massachusetts, United States). The total RNA was later reversed transcribed to cDNA by CellAmp[™] Whole Transcriptome Amplification Kit (TaKaRa, Kyoto, Japan).

primers were designed *via* the Primer Premier 5.0 (Premier Biosoft, San Francisco, United States) and the Primer-BLAST of NCBI (ncbi.nlm.nih.gov/tools/primer-blast/) (Ye et al., 2012).

The PCR products separated by gel electrophoresis was excised, purified, and cloned into the pMD19-T vector (TaKaRa, Kyoto, Japan) prior to the Sanger sequencing by a commercial service provider (GENEWIZ, Suzhou, China).

2.6 Bioinformatics analyses

The open reading frame (ORF) was predicted by the ORF finder (<https://www.ncbi.nlm.nih.gov/orffinder/>) (Misener and Krawetz, 2000). The signal peptide was predicted using SignalP 5.0 Server (<https://services.healthtech.dtu.dk/service.php?SignalP-5.0>) (Almagro Armenteros et al., 2019). Further,

the N-glycosylation motif was predicted by the NetNGlyc 1.0 Server (<https://services.healthtech.dtu.dk/service.php?NetNGlyc-1.0>) (Gupta and Brunak, 2002), the O-terminal glycosylation site was predicted by the NetNGlyc 1.0 Server (<https://services.healthtech.dtu.dk/service.php?NetOGlyc-4.0>) (Steentoft et al., 2013). The cysteine (Cys) residues and putative disulfide bonds were predicted *via* the DiANNA 1.1 web server (<http://clavius.bc.edu/~clotelab/DiANNA/>) (Ferre and Clote, 2005). The secondary structure was predicted by the NovoPro software (<https://www.novopro.cn/tools/secondary-structure-prediction.html>) (Jones, 1999), and the SWISS-PROT software was used to analyze the tertiary spatial structure (<https://swissmodel.expasy.org/>) (Bairoch and Boeckmann, 1991). The conserved domain was detected by the SMART software (<http://smart.embl-heidelberg.de/>) (Letunic and Bork, 2018).

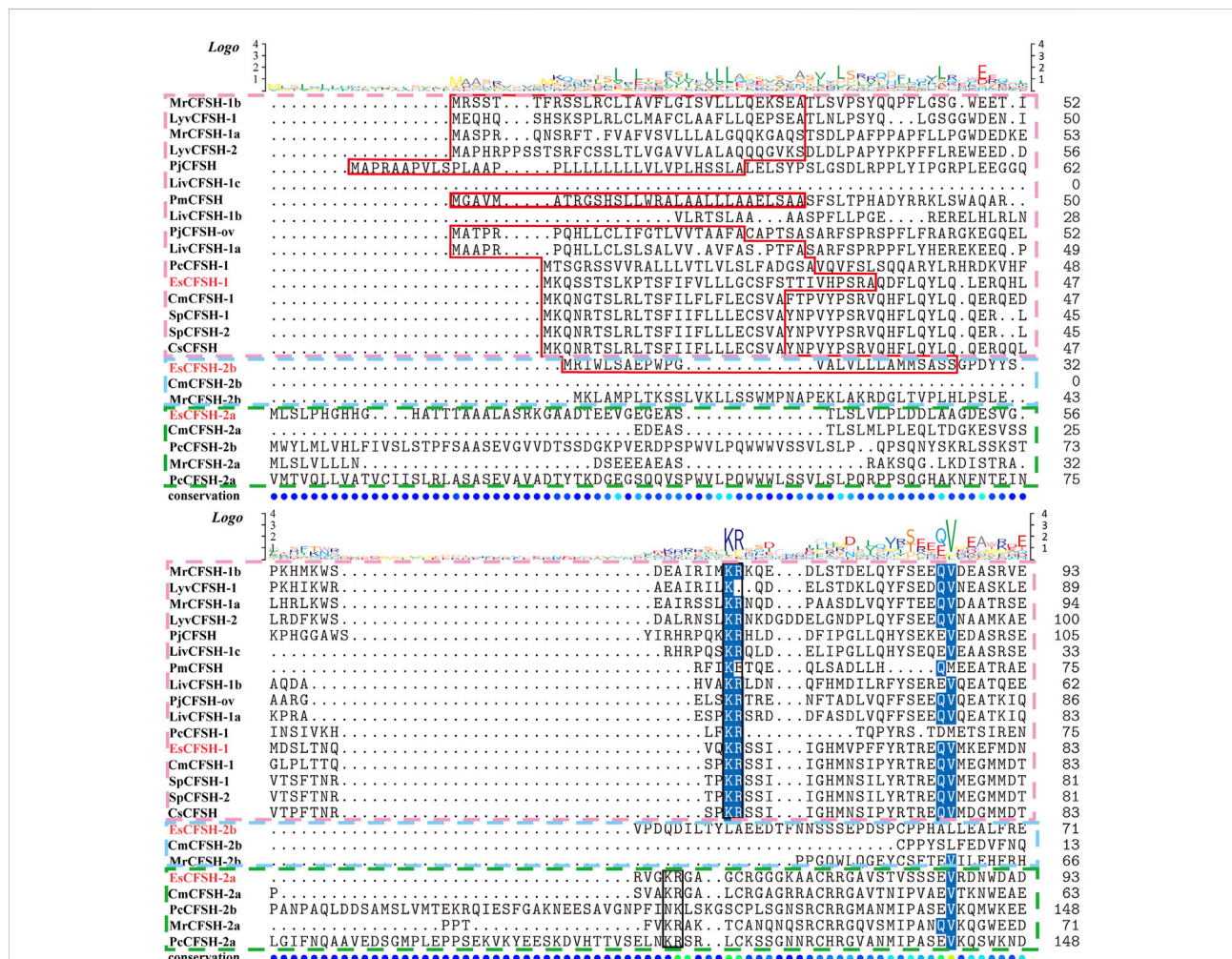
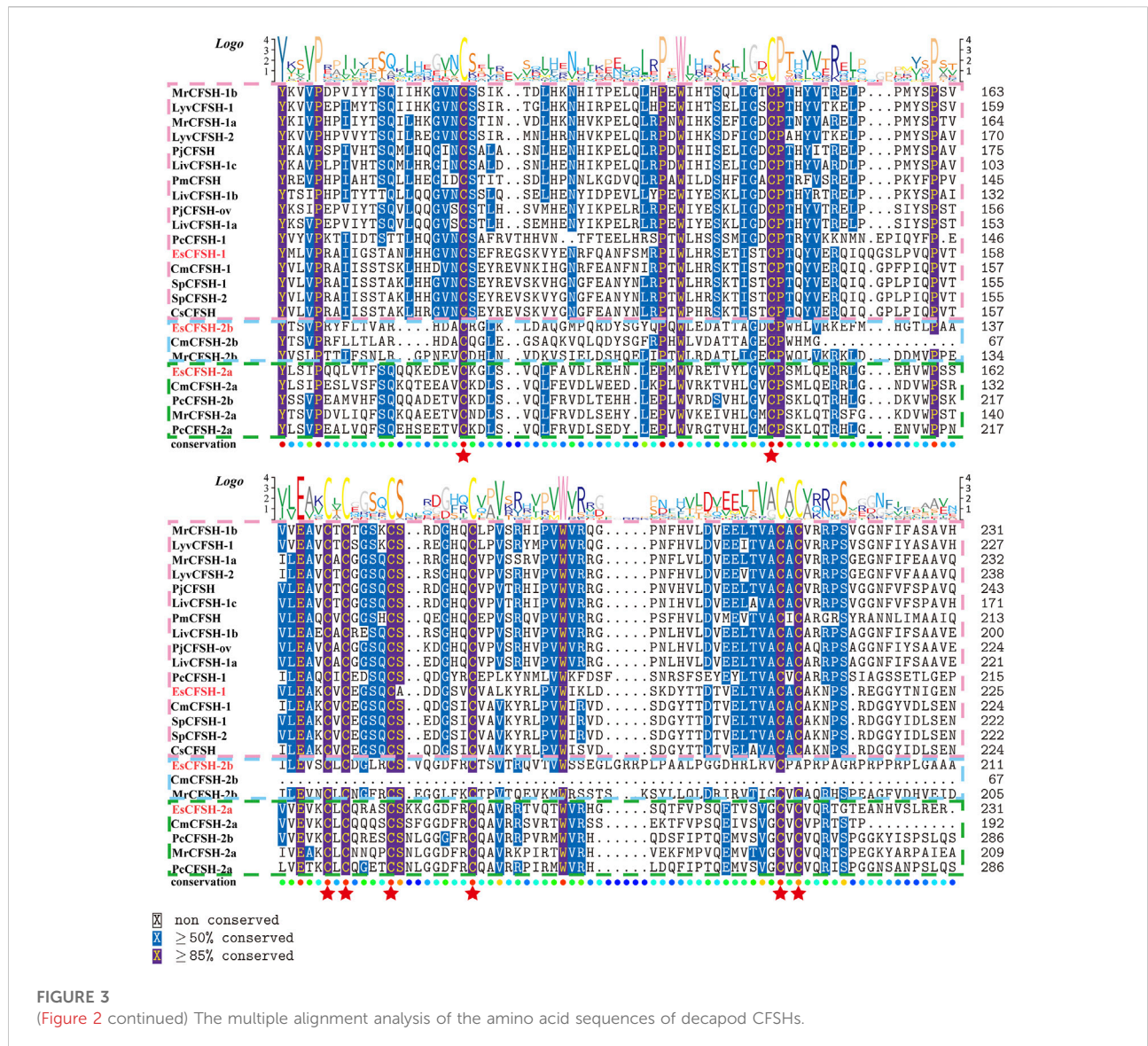


FIGURE 2
The multiple sequence alignment analysis of the amino acid of decapod CFSHs. Three subtypes of CFSHs were boxed, the pink box was CFSH 1, the light blue was CFSH 2b, and the green was CFSH 2a. The signal peptide was outlined by the red frame, and the cleavage site was boxed in black line, the conserved cysteine residues were marked with red stars.

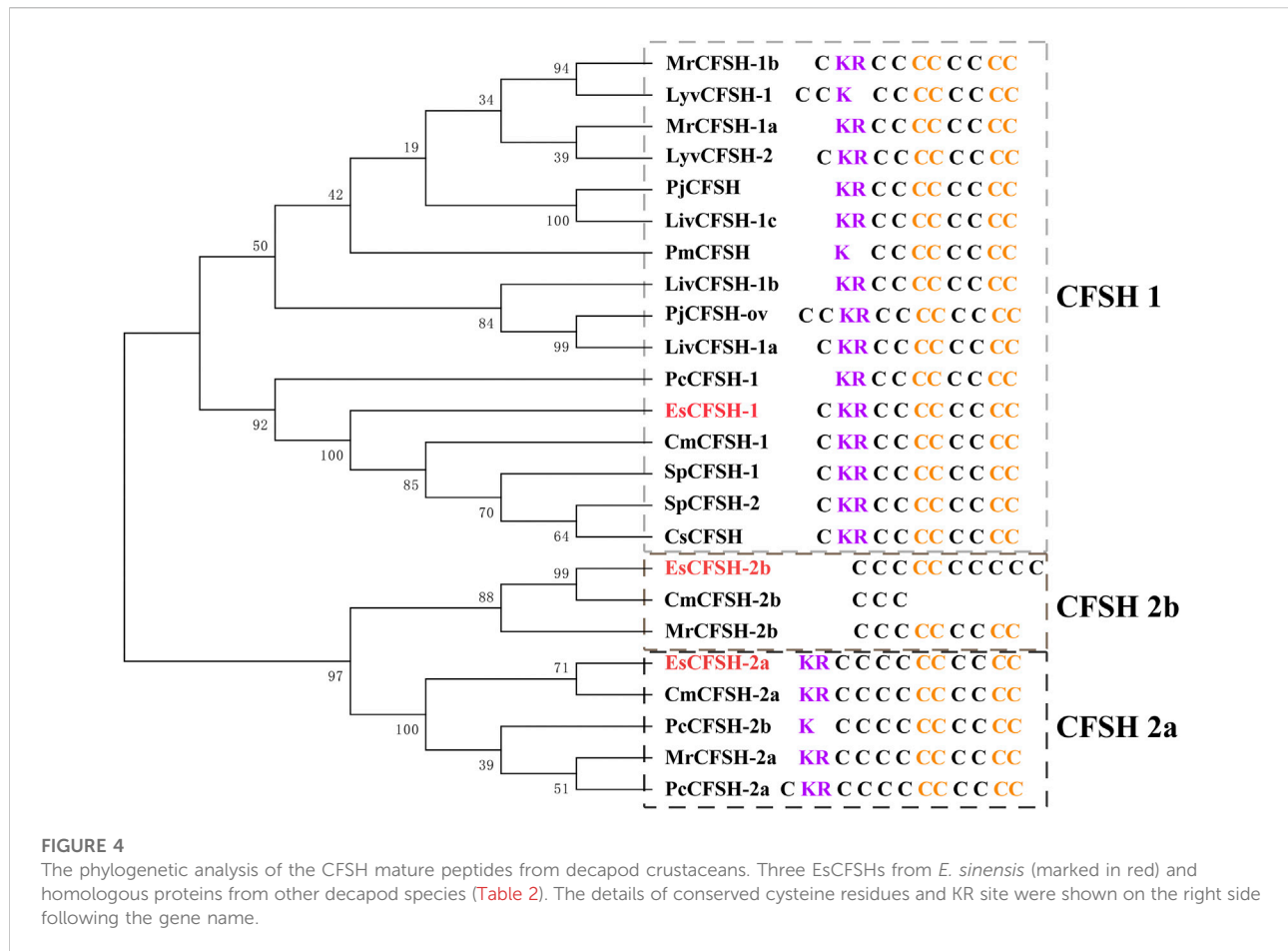


The multiple alignment of full-length amino acid sequences was performed by the ClustalX software using the published CFSH sequences (Table 2) excluding the signal peptide. The phylogenetic tree was constructed using the complete CFSH sequences by the MEGA6 software, in which the neighbor-joining algorithm with 2,000 bootstrap replicates was applied based on the JTT matrix-based model (Saitou and Nei, 1987).

2.7 The preparation of short interfering double-stranded RNA

The synthesis of short interfering double-stranded RNA (dsRNA) was performed using the TranscriptAid™ T7 high yield transcription

kit (Thermo Scientific Inc., Massachusetts, United States) following the standard protocols on the manual. Primers EsCFSH-1-dsF/dsR and EsIAG-dsF/dsR (Table 1) were designed to amplify cDNA fragments of *EsCFSH-1* and *EsIAG* (GenBank ID: KU724192.1) to constructed the recombinant plasmids of pGEM-T-EsCFSH-1 and pGEM-T-EsIAG, respectively. Primers of EGFP-dsF/dsR (Table 1) were used to amplify the fragments of enhanced green fluorescent protein (*EGFP*) gene (GenBank: U55761) to constructed pGEM-T-EGFP. The recombinant plasmids with target genes were used to get the linearized DNA templates, then the RNA transcripts can be generated from 1ug DNA templates. After extraction and purification, dsRNA could be obtained, and the concentration was measured by Nanodrop One (Thermo Scientific Inc., Massachusetts, United States) and stored at -80 °C until use.



Before the application of RNA interference, the dsRNA was diluted with the artificial crab saline (ACS: 2.570 g NaCl, 0.084g KCl, 0.148 g CaCl₂, 0.248g MgCl₂, 0.327 g Na₂SO₄, 0.238 g HEPES solved in 100 ml distilled water).

2.8 The gene knockdown for adult crabs

For adult crabs (body weight: 95.41 ± 10.14 g), four groups were assigned to the experiment of gene knockdown. Each group consisted of eight adult crabs (1:1 sex ratio). For the group of *IAG* or *CFSH-1* knockdown, the dsRNA of *EsIAG* or *EsCFSH-1* was injected into the hemolymph through the arthroal membrane between the third and fourth pleopod by a 100 μL micro syringe (Shanghai Anting, Shanghai, China). For the group of blank or negative control, the equivalent amount of artificial crab saline (ACS) or dsRNA *EGFP* was injected. The quantity of delivered dsRNA was 1 μg per each gram of the body weight. Tissue samples including EG and AG of each crab were collected for RNA extraction 24 h after the RNA interference.

2.9 The gene knockdown for juvenile crabs

For the gene knockdown for juvenile crabs, 150 individuals at the stage of juvenile I were injected with dsRNA *EsCFSH-1* (2 μg per 1 g of body weight) using the IM11-2 and M-152 micro injection system (NARISHIGE, Tokyo, Japan). In the control group, the juveniles were injected with the equivalent amount of ACS. The samples were collected at the stage of juvenile III (around 15 days). The whole bodies of juvenile crabs were fixed in the PBS with 4% paraformaldehyde for the morphological observation.

2.10 The morphological observation of external reproductive structures

The gross anatomy of the male and female juveniles was observed under an Olympus SZ51 stereomicroscope (Olympus, Shinjuku, Japan). For the scanning electron microscopical observation, the samples were prepared through ethanol

gradient dehydration and tert-butyl alcohol replacement. After being frozen for 20 h in -20°C , the samples were dried for 24 h in the Martin Christ Alpha 1-4LD plus freeze-dryer (Martin Christ, Osterode, Germany) before being sprayed with gold by a Hitachi E-1010 ion sputtering device (Hitachi, Tokyo, Japan). The micrographs were taken using a Hitachi S-3400N scanning electron microscope (Hitachi, Tokyo, Japan).

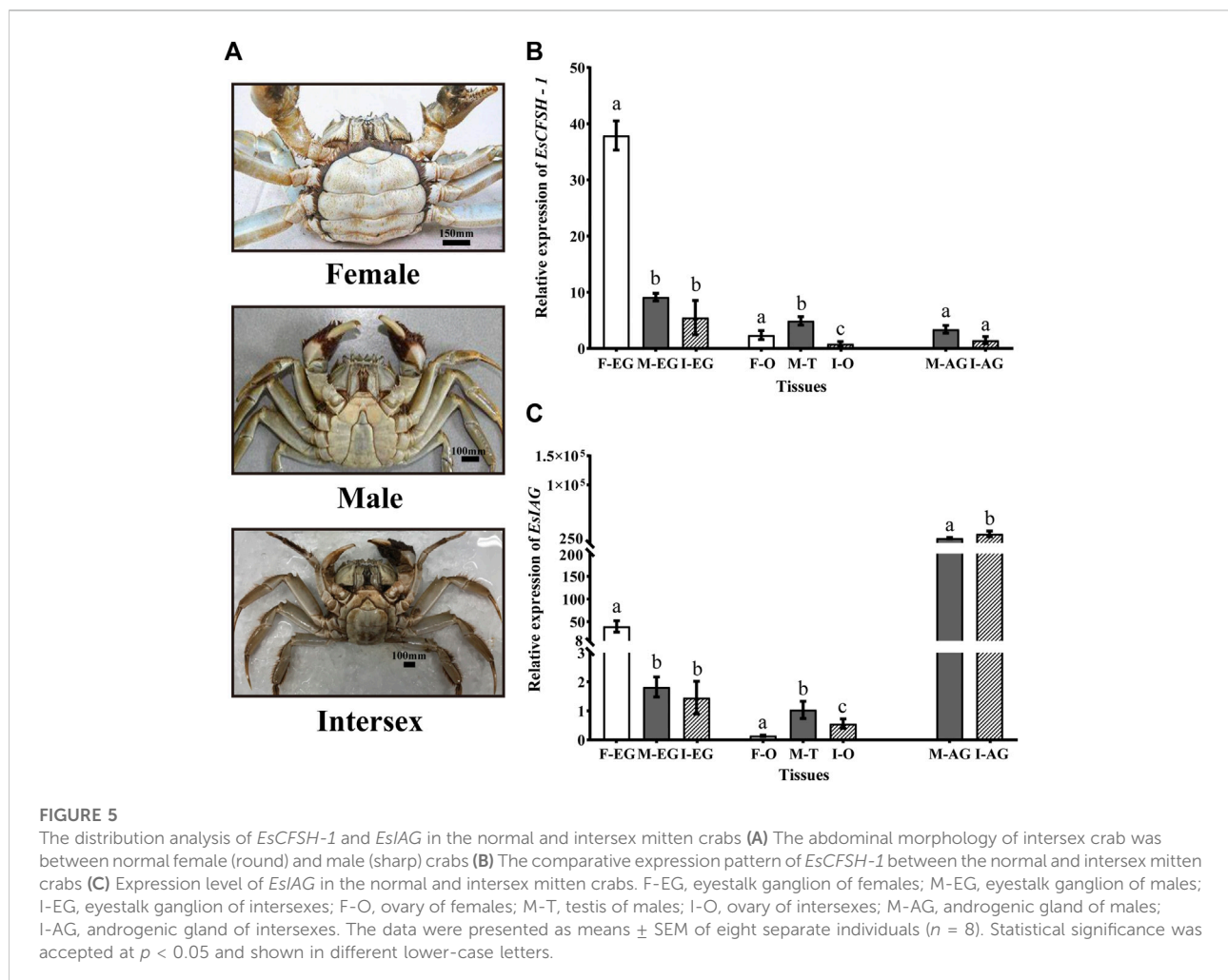
2.11 Quantitative real-time PCR

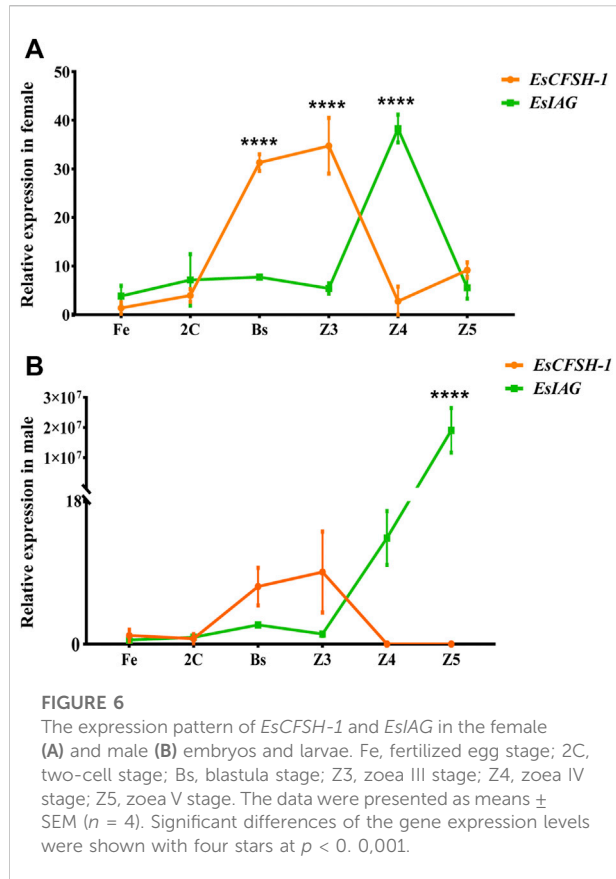
The fluorescence quantitative real-time PCR (qRT-PCR) was performed using the 7,500 Real-Time PCR system (Applied Biosystems, California, United States) with TB Green Premix Dimer Eraser (2x) (TaKaRa, Kyoto, Japan). The qRT-PCR was carried out in a total volume of 20 μL , containing 10 μL TB Green Premix Dimer Eraser (2x), 2 μL diluted cDNA, 0.5 μL forward/reverse primers (1 mM), 0.4 μL ROX Reference Dye II and 6.4 μL RNase-free water. The PCR program included the initial denaturation at 95°C for 30 s, followed by 40 cycles of

denaturation at 95°C for 15 s, annealing and elongation at 60°C for 15 s and 72°C for 30 s. Each sample was run in triplicates. All primers used for the qRT-PCR were listed in Table 1. A standard curve was used to calculate the amplification efficiency and ensure primer specificity of each primer pair, *EsCFSH-1*-qF/R had the amplification efficiency of 105.895%, *EsIAG*-qF/R had the amplification efficiency of 101.054%, and the amplification efficiency of *Es- β -actin*-qF/R was 100.451%. The relative expression levels of target genes were calculated by the $2^{-\Delta\Delta\text{Ct}}$ method (Livak and Schmittgen, 2001) using *Es- β -actin* (GenBank ID: ATO74508.1) as the reference gene.

2.12 Statistical analysis

The normality of data was established by the Kolmogorov-Smirnov test. All the data were presented in a normal distribution and tested for variances homogeneity by the Levene's test. The statistical analysis was performed by the one-way ANOVA followed by Tukey's multiple tests using the GraphPad Prism



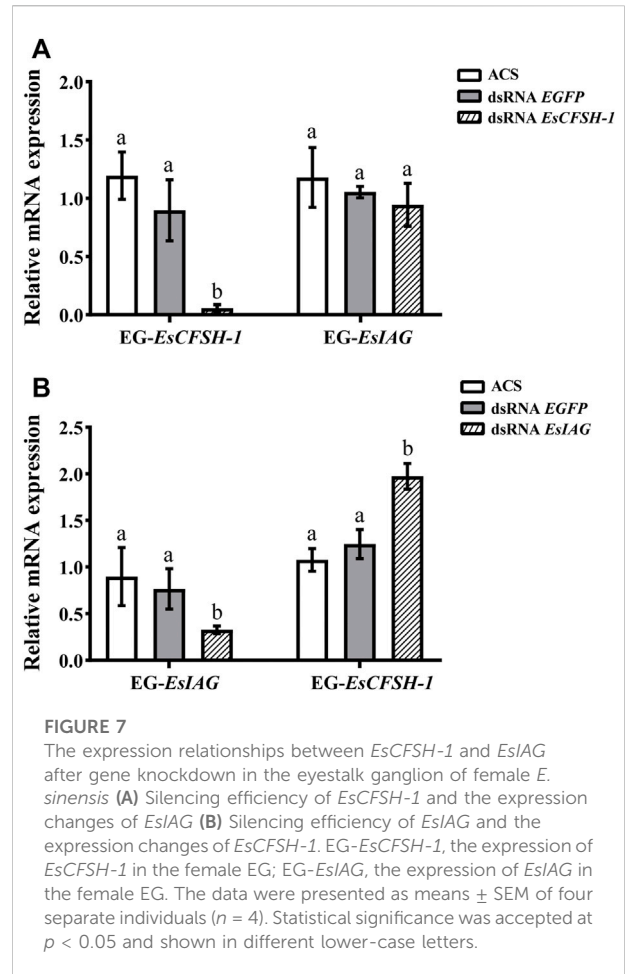


seven software (GraphPad Software, San Diego, United States) (Stoline, 1981; Swift, 1997). The quantitative results were represented as mean \pm SEM.

3 Results

3.1 The bioinformatics prediction of full length *EsCFSH-1* gene and protein

The full-length cDNA of *EsCFSH-1* (GenBank ID: OP351640) had 903 bp, included a 73-nt 3' UTR, a 149-nt 5' UTR, and the 681-nt ORF that encoded a protein of 226 amino acid residues (Figure 1A). The CFHS preprohormone was comprised of a signal peptide of 34 residues, a CFHS-precursor related peptide of 22 residues, a dibasic processing signal (Lys-Arg, KR), and a mature peptide of 168 residues. The molecular weight of the *EsCFSH-1* protein was 25.68 kDa, and the theoretical isoelectric point was 8.06. The instability coefficient of the protein was 40.4. The average hydrophilic coefficient of the protein was -0.269. The mature peptide had a single conserved N-glycosylation site (Asn-Cys-Ser, NCS) at N103 and two O-glycosylation sites at S136 and T140. Eight cysteine residues were predicted to form four intramolecular

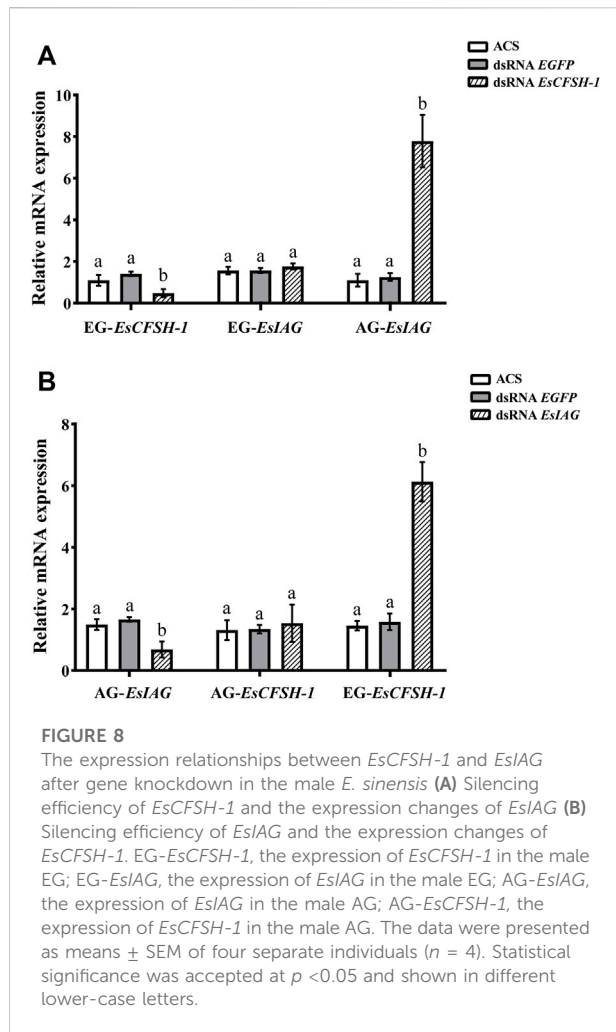


disulfide bridges: C104-C209, C138-C171, C164-C178, and C166-C207.

The secondary structure of *EsCFSH-1* contained 82 α -helices (45.79%), 12 β -turns (5.31%), 100 random coils (44.25%), and 32 extended strands (14.16%) (Figure 1B). The domains detected by SMART showed that *EsCFSH-1* had a signal peptide and an interleukin-17 (IL-17) domain (Figure 1C). The prediction of 3D structure showed the *EsCFSH-1* could form a “butterfly” like homodimer (Figure 1D).

3.2 The phylogenetic analysis of *EsCFSH-1*

By the comparison of amino acid sequences, the CFHSs of decapods could be categorized into three subtypes: type 1, type 2a, and type 2b (Figures 2, 3). The difference between type 1 and type 2 reflected on the existence of the signal peptide, while the difference between type 2a and type 2b reflected on the existence of the KR site. Additionally, the type 2b CFHSs contained two extra cysteine residues at the N-terminal and no N-glycosylation sites. The similarity between SpCFSH-1 and *EsCFSH-1* was



68.9%, which was the highest among the compared CFSH sequences. Based on the sequence of 24 published CFSH mature peptides (Table 2), the phylogenetic tree confirmed that there were two main subtypes of CFSHs (Figure 4). In conclusion, *EsCFSH-1* belonged to the type 1 CFSH.

3.3 The tissue expression of *EsCFSH-1* and *EsIAG* between the normal and intersex crabs

The abdomens of the intersex crabs exhibited an intermediate shape comparing to the narrow shape of male and the broad shape of female (Figure 5A). Each intersex crab possessed the female reproductive organ ovary and the male reproductive organ vas deferens attached by the androgenic gland despite it was genetically tested as female.

For *EsCFSH-1*, although it was expressed in AG and gonads, the main expression tissue was EG, and the expression in EG

showed the higher level in the normal female crabs than the intersex crabs ($p < 0.05$) and males ($p < 0.05$) (Figure 5B).

Furthermore, for *EsIAG*, the expression in AG showed the higher level in the intersex crabs than the normal males ($p < 0.05$) (Figure 5C). Besides, the EG of the normal females had the higher expression level than the males and even the intersex crabs ($p < 0.05$) (Figure 5C).

3.4 The temporal comparison of *EsCFSH-1* and *EsIAG* expression in the embryos and larvae

For the sex-distinguished embryo and larva (Figures 6A,B), the expression levels of *EsCFSH-1* and *EsIAG* both were low in the early stages of development (Fe and 2C), and then *EsCFSH-1* was higher expressed than *EsIAG* at the stages of Bs and Z3 ($p < 0.0001$), while the expressed pattern of *EsCFSH-1* and *EsIAG* was reversed between the Z3 and Z4 stage. After the Z4 stage, the expression of *EsIAG* surged and *EsCFSH-1* declined sharply in male larva ($p < 0.0001$), the trend was opposite in female larva.

3.5 The regulatory feedback loop between *EsCFSH-1* and *EsIAG*

For the female crabs, the inhibition rate of *EsCFSH-1* expression was 89% after *EsCFSH-1* knockdown ($p < 0.05$), and the expression of *EsIAG* in EG had no change (Figure 7A). Furthermore, the inhibition rate of *EsIAG* expression was 71% after *EsIAG* knockdown ($p < 0.05$), and the expression of *EsCFSH-1* in EG rose significantly compared with the ACS and dsRNA *EGFP* groups ($p < 0.05$) (Figure 7B).

For the male crabs, the expression of *EsCFSH-1* significantly decreased by 68% ($p < 0.05$) after injecting with dsRNA *EsCFSH-1* in EG, and the expression of *EsIAG* in EG had no change, but a significant rising occurred in male AG ($p < 0.05$) (Figure 8A). After the knockdown of *EsIAG*, the expression of *EsIAG* in AG decreased significantly by 62% ($p < 0.05$), the expression of *EsCFSH-1* did not change in male AG, while it increased significantly in male EG ($p < 0.05$) (Figure 8B).

To sum results up, there was a repression function from *EsCFSH-1* to *EsIAG* in female and male EGs, conversely, the inhibiting effect from *EsIAG* to *EsCFSH-1* only existed in male AG.

3.6 The impact of *EsCFSH-1* knockdown on the sexual phenotype

The knockdown of *EsCFSH-1* at the stage of juvenile I could not skew the sex ratio. For the crabs survived to the stage of juvenile III, there were 12 females and 13 males with a sex ratio of nearly 1:1 which was similar to the sex ratio of the control group (Figure 9A).

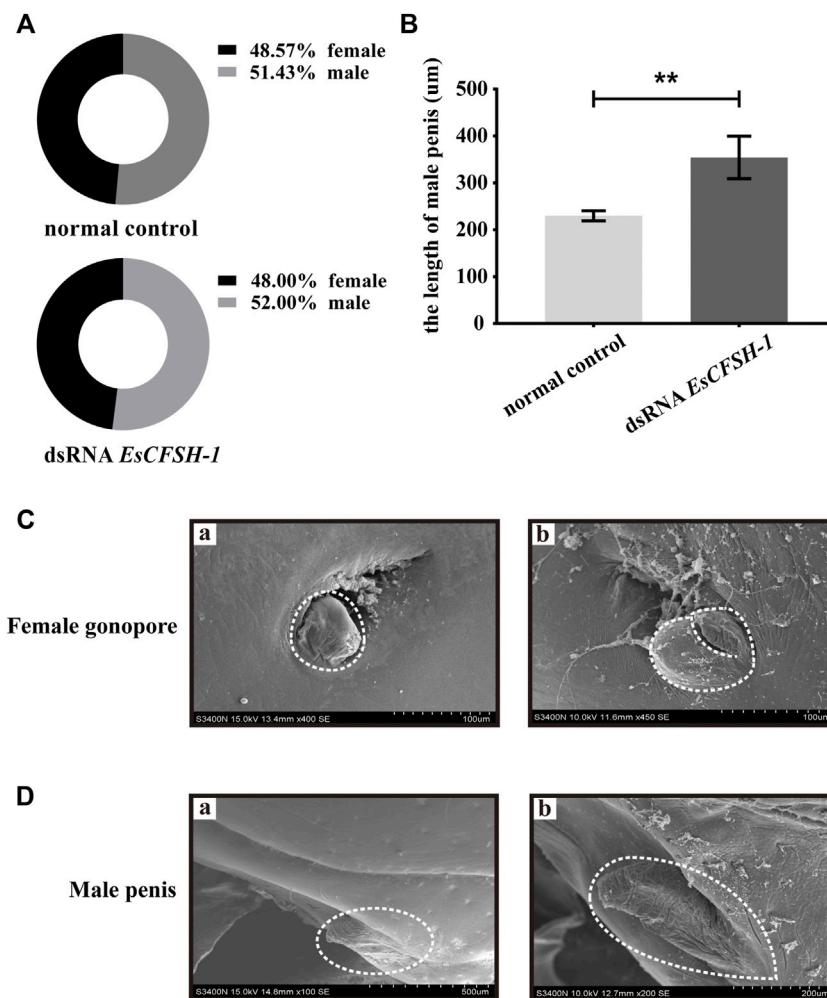


FIGURE 9

The female and male sexual characteristics of juvenile *E. sinensis* after *EsCFSH-1* knockdown (A) Sexual ratio of normal control group and dsRNA *EsCFSH-1* group (B) The length of male penis (μm). The data were presented as means \pm SEM of four separate individuals ($n = 3$), and the double-stars indicated $p < 0.01$ (C) The female gonopore characteristics before (A) and after (B) treated dsRNA *EsCFSH-1* (D) The male penis characteristics before (A) and after (B) treated dsRNA *EsCFSH-1*.

However, the knockdown of *EsCFSH-1* appeared to have an impact on the development of external reproductive structures. The penis of a male juvenile became 140% larger after the treatment (Figures 9B,D), while the cover of female gonopore developed into an abnormal cleft structure in several cases (Figure 9C).

4 Discussion

EsCFSH-1 identified from genome of *E. sinensis* shared the typical protein structures of the type 1 CFSHs, including a signal peptide, a KR site, an IL-17 domain, and eight highly conserved cysteine residues. By comparison, the CFSH-2b subtype had the signal peptide but no KR site, while the CFSH-2a had the KR site but no signal peptide.

The signal peptide is necessary for the translocation of protein *via* the conventional secretory pathway (Rabouille, 2017). Therefore, CFSH-1 and 2b should belong to the secretory proteins, being transported to the plasma membrane through the endoplasmic reticulum and Golgi apparatus by COPII-coated vesicles (Palade, 1975; Brough et al., 2017). Based on the IL-17 domain, it is presumed that CFSH-1 participates in the cellular process of signal transduction. The protein with the IL-17 domain could mediate tyrosine phosphorylation to activate the JAK/STAT signaling pathway which transmits biochemical signals from IL-17 receptors to the nucleus of the regulated cell (Cooper and Adunyah, 1999). The KR site is important for the formation of mature protein of CFSH-1. It has been reported that the endocrine cells synthesize the peptide hormone by endoproteolysis of the precursor peptide at the site of Lys-Arg (KR) or Arg-Arg (RR)

after the cleavage of the signal peptide (Hosaka et al., 1991; Veenstra, 2000).

Compared to the normal crabs, we found that the intersex crabs show the aberrant expression of *EsCFSH-1* and *EsIAG*. Normally, *CFSH-1* expressed at the highest level in the female EG (Kotaka and Ohira, 2017; Liu et al., 2018; Liu et al., 2021a) and *IAG* extremely highly expressed in the male specific organ AG (Sagi and Aflalo, 2005). For the intersex crabs, the expression of *EsCFSH-1* and *EsIAG* in the EG and AG was close to the male level. Given these intersex crabs are genetic females, the masculinized phenotype may be related to the lowered *EsCFSH-1* expression and the increased *EsIAG* expression, which eventually lead to the unorthodox emergence of AG. Furthermore, as the demethylation of 5'-UTR region of *CFSH* ensured the high expression of *CFSH* in the female EG (Jiang et al., 2020a), our ongoing study will find out whether an abnormally high methylation of this region decrease the expression of *EsCFSH-1* in the intersex crabs.

Next, we examined the role of *EsCFSH-1* and *EsIAG* in the process of sexual sex differentiation. Based on our results, it seems that *EsCFSH-1* initiates feminization by an effective repression of *EsIAG* expression since the late stage of embryogenesis. In the male perspective, the early repression of *EsIAG* appears inefficient, which results in the surge of *EsIAG* expression during the transition after Z4 to megalopa. In a word, the change trends of the two genes were almost same before the Z4 stage, at which could be confirmed as the key period when the feedback loop relationship between *EsCFSH-1* and *EsIAG* worked. Our finding is consistent with the morphological observation of *Eriocheir japonicus*, in which the sexual differentiation of internal reproductive organ (gonoduct) could not be observed until the megalopa stage (Lee et al., 1994).

The experiment of gene knockdown was later conducted to figure out the regulatory relationship between *EsCFSH-1* and *EsIAG*. Our results confirmed the inhibitory effect of *EsCFSH-1* to *EsIAG* in the AG, which agree with the finding in the mud crab *S. paramamosain* (Liu et al., 2018). We also found the inhibitory effect of *EsIAG* to *EsCFSH-1* in the EG of male and female, which is supported by the finding in the peppermint shrimp *L. vittate* (Liu et al., 2021a; Liu et al., 2021c). Our study confirmed the existence of the regulatory feedback loop between *EsCFSH-1* and *EsIAG*. In *S. paramamosain*, *CFSH* negatively regulated *IAG* by inhibiting *STAT* (signal transducers and activators of transcription), which was a key transcription factor of *IAG* (Jiang et al., 2020c). Further studies are required to verify the inhibitory mechanism of *CFSH* to *IAG* in male *E. sinensis* and more importantly investigate the inhibitory mechanism of *IAG* to *CFSH*.

Our study also revealed that *EsCFSH-1* regulates the development of reproductive system during the sexual sex differentiation. The disruption of *EsCFSH-1* expression could lead to the deformed cover of female gonopores and the elongation of male penises of juveniles. The impaired development of female gonopores was also observed in *C. sapidus* (Zmora and Chung, 2014) and *S. paramamosain* (Jiang et al., 2020b) after the *CFSH*

knockdown in juvenile females. As the positive correlation has been well established between the *IAG* expression and the development of male sex characteristics (Khalaila et al., 2001), the over-growth of penis should be explained by the compromised inhibitory effect of *EsCFSH-1* to *EsIAG*.

In summary, we compared the gene expression of *EsCFSH-1* and *EsIAG* between normal and intersex crabs, and between sex-distinguished embryos and larvae at various developmental stages. Next, we confirmed the existence of the regulatory feedback loop between *EsCFSH-1* and *EsIAG*. At last but not least, we demonstrated the relationship between *EsCFSH-1* and the development of reproductive system. Our study provides strong evidence for the feminization function of *CFSH-1*, which contributes to a better understanding of the molecular mechanism of sexual sex differentiation.

Data availability statement

The datasets presented in this study can be found in online repositories. The names of therepository/repositories and accession number(s) can be found below: <https://www.ncbi.nlm.nih.gov/genbank/>, OP351640.

Author contributions

DZ: experimental design, manuscript writing, experiment conducting, data analysis TF: experimental design, data analysis NM: experiment conducting WL: experiment conducting RH: data analysis SS: experiment conducting ZC: experimental design, fundraising, supervision.

Funding

The work was supported by the National Natural Science Foundation of China (32072964), the National Key R and D Program of China (2018YFD0900303), and the Ten Thousand Talents Program.

Acknowledgments

We would like to thank the anonymous reviewers for their helpful remarks and suggestions.

Conflict of interest

The authors declare that they have no known competing financial interests or personal relationships that could have appeared to influence the work reported in this paper.

Publisher's note

All claims expressed in this article are solely those of the authors and do not necessarily represent those of their affiliated

organizations, or those of the publisher, the editors and the reviewers. Any product that may be evaluated in this article, or claim that may be made by its manufacturer, is not guaranteed or endorsed by the publisher.

References

- Adkins-Regan, E. (2014). A new hormone negates a default principle. *Endocrinology* 155, 10–11. doi:10.1210/en.2013-2078
- Almagro Armenteros, J. J., Tsirigos, K. D., Sonderby, C. K., Petersen, T. N., Winther, O., Brunak, S., et al. (2019). SignalP 5.0 improves signal peptide predictions using deep neural networks. *Nat. Biotechnol.* 37, 420–423. doi:10.1038/s41587-019-0036-z
- Bairoch, A., and Boeckmann, B. (1991). The SWISS-PROT protein sequence data bank. *Nucleic Acids Res.* 19, 2247–2249. doi:10.1093/nar/19.suppl.2247
- Brough, D., Pelegrin, P., and Nickel, W. (2017). An emerging case for membrane pore formation as a common mechanism for the unconventional secretion of FGF2 and IL-1 β . *J. Cell. Sci.* 130, 3197–3202. doi:10.1242/jcs.204206
- Cooper, S. V. S. R. S., and Adunyah, S. E. (1999). Evidence for the involvement of JAK STAT pathway in the signaling mechanism of interleukin-17. *Biochem. Biophys. Res. Commun.* 262, 14–19. doi:10.1006/bbrc.1999.1156
- Cui, Z., Du, J., Yang, Y., and Liu, Y. (2018). A specific molecular marker for identifying the sex of *Eriocheir sinensis*. *China Pat. Appl.* 4, 201811449018.
- Cui, Z., Liu, Y., Yuan, J., Zhang, X., Ventura, T., Ma, K. Y., et al. (2021). The Chinese mitten crab genome provides insights into adaptive plasticity and developmental regulation. *Nat. Commun.* 12, 2395. doi:10.1038/s41467-021-22604-3
- Farhadi, A., Cui, W., Zheng, H., Li, S., Zhang, Y., Ikhwanuddin, M., et al. (2021). The regulatory mechanism of sexual development in decapod Crustaceans. *Front. Mar. Sci.* 8, 679687. doi:10.3389/fmars.2021.679687
- Ferre, F., and Clote, P. (2005). DiANNA: A web server for disulfide connectivity prediction. *Nucleic Acids Res.* 33, 230–232. doi:10.1093/nar/gki412
- Fu, C., Li, F., Wang, L., Wu, F., Wang, J., Fan, X., et al. (2020). Molecular characteristics and abundance of insulin-like androgenic gland hormone and effects of RNA interference in *Eriocheir sinensis*. *Anim. Reprod. Sci.* 215, 106332. doi:10.1016/j.anireprosci.2020.106332
- Gupta, R., and Brunak, S. (2002). Prediction of glycosylation across the human proteome and the correlation to protein function. *Pac. Symp. Biocomput.* 7, 310–322.
- Hosaka, M., Nagahama, M., Kim, W. S., Watanabe, T., Hatsuzawa, K., Ikemizu, J., et al. (1991). Arg-X-Lys/Arg-Arg motif as a signal for precursor cleavage catalyzed by furin within the constitutive secretory pathway. *J. Biol. Chem.* 266, 12127–12130. doi:10.1016/s0021-9258(18)98867-8
- Jiang, Q., Lin, D., Huang, H., Wang, G., and Ye, H. (2020a). DNA methylation inhibits the expression of CFSH in mud crab. *Front. Endocrinol.* 11, 163. doi:10.3389/fendo.2020.00163
- Jiang, Q., Lu, B., Lin, D., Huang, H., Chen, X., and Ye, H. (2020b). Role of crustacean female sex hormone (CFSH) in sex differentiation in early juvenile mud crabs, *Scylla paramamosain*. *Gen. Comp. Endocrinol.* 289, 113383. doi:10.1016/j.ygcen.2019.113383
- Jiang, Q., Lu, B., Wang, G., and Ye, H. (2020c). Transcriptional inhibition of sp-IAG by Crustacean female sex hormone in the mud crab, *Scylla paramamosain*. *Int. J. Mol. Sci.* 21, 5300. doi:10.3390/ijms21155300
- Jones, D. T. (1999). Protein secondary structure prediction based on position-specific scoring matrices. *J. Mol. Biol.* 292, 195–202. doi:10.1006/jmbi.1999.3091
- Khalaila, I., Katz, T., Abdu, U., Yehzekel, G., Sagi, A., and Sagi, A. (2001). Effects of implantation of hypertrophied androgenic glands on sexual characters and physiology of the reproductive system in the female red claw crayfish, *Cherax quadricarinatus*. *Gen. Comp. Endocrinol.* 121, 242–249. doi:10.1006/gcen.2001.7607
- Kotaka, S., and Ohira, T. (2017). cDNA cloning and *in situ* localization of a crustacean female sex hormone-like molecule in the kuruma prawn *Marsupenaeus japonicus*. *Fish. Sci.* 84, 53–60. doi:10.1007/s12562-017-1152-7
- Lee, T.-H., Yamauchi, M., and Yamazaki, F. (1994). Sex differentiation in the crab *Eriocheir japonicus* (Decapoda, Grapsidae). *Invertebr. Reproduction Dev.* 25, 123–137. doi:10.1080/07924259.1994.9672377
- Leticia, I., and Bork, P. (2018). 20 years of the SMART protein domain annotation resource. *Nucleic Acids Res.* 46, D493–D496. doi:10.1093/nar/gkx922
- Levy, T., Rosen, O., Simons, O., Alkalay, A. S., and Sagi, A. (2017). The gene encoding the insulin-like androgenic gland hormone in an all-female parthenogenetic crayfish. *PLoS ONE* 12, e0189982. doi:10.1371/journal.pone.0189982
- Levy, T., and Sagi, A. (2020). The "IAG-Switch"-A key controlling element in decapod Crustacean sex differentiation. *Front. Endocrinol.* 11, 651. doi:10.3389/fendo.2020.00651
- Levy, T., Tamone, S. L., Manor, R., Aflalo, E. D., Sklarz, M. Y., Chalifa-Caspi, V., et al. (2020). The IAG-switch and further transcriptomic insights into sexual differentiation of a protandric shrimp. *Front. Mar. Sci.* 7, 587454. doi:10.3389/fmars.2020.587454
- Liang, X., Yan, S., Zheng, C., and Guo, D. (1974). The larval development of *Eriocheir sinensis* H. milne Edwards. *ACTA ZOOL. SIN.* 20, 61–75.
- Liu, A., Liu, J., Liu, F., Huang, Y., Wang, G., and Ye, H. (2018). Crustacean female sex hormone from the mud crab *Scylla paramamosain* is highly expressed in prepubertal males and inhibits the development of androgenic gland. *Front. Physiol.* 9, 924. doi:10.3389/fphys.2018.00924
- Liu, F., Shi, W., Huang, L., Wang, G., Zhu, Z., and Ye, H. (2021a). Roles of Crustacean female sex hormone 1a in a protandric simultaneous hermaphrodite shrimp. *Front. Mar. Sci.* 8, 791965. doi:10.3389/fmars.2021.791965
- Liu, F., Shi, W., Ye, H., Liu, A., and Zhu, Z. (2021b). RNAi reveals role of insulin-like androgenic gland hormone 2 (IAG2) in sexual differentiation and growth in hermaphrodite shrimp. *Front. Mar. Sci.* 8, 666763. doi:10.3389/fmars.2021.666763
- Liu, F., Shi, W., Ye, H., Zeng, C., and Zhu, Z. (2021c). Insulin-like androgenic gland hormone 1 (IAG1) regulates sexual differentiation in a hermaphrodite shrimp through feedback to neuroendocrine factors. *Gen. Comp. Endocrinol.* 303, 113706. doi:10.1016/j.ygcen.2020.113706
- Livak, K. J., and Schmittgen, T. D. (2001). Analysis of relative gene expression data using real-time quantitative PCR and the 2^{- $\Delta\Delta C_T$} Method. *METHODS* 25, 402–408. doi:10.1006/meth.2001.1262
- Misener, S., and Krawetz, S. A. (2000). *Bioinformatics methods and protocols*. Totowa, NJ: Humana.
- Montú, M., Anger, K., and De Bakker, C. (1996). Larval development of the Chinese mitten crab *Eriocheir sinensis* H. Milne-edwards (Decapoda: Grapsidae) reared in the laboratory. *Helgol. Meeresunters.* 50, 223–252. doi:10.1007/BF02367153
- Palade, G. (1975). Intracellular aspects of the process of protein synthesis. *Science* 189, 347–358. doi:10.1126/science.1096303
- Priyadarshi, H., Das, R., Pavan-Kumar, A., Gireesh-Babu, P., Javed, H., Kumar, S., et al. (2017). Silencing and augmentation of IAG hormone transcripts in adult *Macrobrachium rosenbergii* males affects morphotype transformation. *J. Exp. Biol.* 220, 4101–4108. doi:10.1242/jeb.163410
- Rabouille, C. (2017). Pathways of unconventional protein secretion. *Trends Cell. Biol.* 27, 230–240. doi:10.1016/j.tcb.2016.11.007
- Sagi, A., and Aflalo, E. D. (2005). The androgenic gland and monosex culture of freshwater prawn *Macrobrachium rosenbergii* (de man): A biotechnological perspective. *Aquac. Res.* 36, 231–237. doi:10.1111/j.1365-2109.2005.01238.x
- Saitou, N., and Nei, M. (1987). The neighbor-joining method a new method for reconstructing phylogenetic trees. *Mol. Biol. Evol.* 4, 406–425. doi:10.1093/oxfordjournals.molbev.a040454
- Song, C., Liu, L., Hui, M., Liu, Y., Liu, H., and Cui, Z. (2018). Primary molecular basis of androgenic gland endocrine sex regulation revealed by transcriptome analysis in *Eriocheir sinensis*. *J. Oceanol. Limnol.* 37, 223–234. doi:10.1007/s00343-019-7254-6
- Stentoft, C., Vakhrushev, S. Y., Joshi, H. J., Kong, Y., Vester-Christensen, M. B., Schjoldager, K. T., et al. (2013). Precision mapping of the human O-GalNAc glycoproteome through Simple Cell technology. *EMBO J.* 32, 1478–1488. doi:10.1038/emboj.2013.79

- Stoline, M. R. (1981). The status of multiple comparisons simultaneous estimation of all pairwise comparisons in one-way ANOVA designs. *Am. Statistician* 35, 134–141. doi:10.1080/00031305.1981.10479331
- Swift, M. L. (1997). GraphPad prism, data analysis, and scientific graphing. *J. Chem. Inf. Comput. Sci.* 37, 411–412. doi:10.1021/ci960402j
- Toyota, K., Miyakawa, H., Hiruta, C., Sato, T., Katayama, H., Ohira, T., et al. (2021). Sex determination and differentiation in decapod and cladoceran Crustaceans: An overview of endocrine regulation. *Genes* 12, 305. doi:10.3390/genes12020305
- Tsutsui, N., Kotaka, S., Ohira, T., and Sakamoto, T. (2018). Characterization of distinct ovarian isoform of crustacean female sex hormone in the kuruma prawn *Marsupenaeus japonicus*. *Comp. Biochem. Physiol. A Mol. Integr. Physiol.* 217, 7–16. doi:10.1016/j.cbpa.2017.12.009
- Veenstra, J. A. (2000). Mono- and dibasic proteolytic cleavage sites in insect neuroendocrine peptide precursors. *Archives Insect Biochem. Physiology* 43, 49–63. doi:10.1002/(SICI)1520-6327(200002)43:2<49::AID-ARCH1>3.0.CO;2-M
- Ventura, T., Manor, R., Aflalo, E. D., Weil, S., Rosen, O., and Sagi, A. (2012). Timing sexual differentiation: Full functional sex reversal achieved through silencing of a single insulin-like gene in the prawn, *Macrobrachium rosenbergii*. *Biol. Reprod.* 86, 90–96. doi:10.1095/biolreprod.111.097261
- Ye, J., Coulouris, G., Zaretskaya, I., Cutcutache, I., Rozen, S., and Madden, T. L. (2012). Primer-BLAST: A tool to design target-specific primers for polymerase chain reaction. *BMC Bioinforma.* 13, 134. doi:10.1186/1471-2105-13-134
- Zmora, N., and Chung, J. S. (2014). A novel hormone is required for the development of reproductive phenotypes in adult female crabs. *Endocrinology* 155, 230–239. doi:10.1210/en.2013-1603